MICROMACHINED STIMULATING ELECTRODES

Quarterly Report #7

(Contract NIH-NINDS-N01-NS-2-2379)

April --- June 1994

Submitted to the

Neural Prosthesis Program
National Institute of Neurological Disorders and Stroke
National Institutes of Health

by the

Solid-State Electronics Laboratory
Bioelectrical Sciences Laboratory
Department of Electrical Engineering and Computer Science
University of Michigan
Ann Arbor, Michigan
48109-2122

July 1994

MICROMACHINED STIMULATING ELECTRODES

Summary

During the past quarter, research under this program has focused in several areas. We have continued to produce a variety of passive stimulating probes and provide them to internal and external users. Additional experiments have been performed in penetrating the pia and dura with both single-shank and ten-shank probe structures. Single-shank probes with shallow-diffused (sharp) tips and probes with deep-diffused (blunt) tips both penetrate the pia mater with little discernable cortical dimpling and yield outputs that are below the ability of our present strain-gauge monitoring system to quantify them. None of these probes have successfully penetrated dura mater since their present thicknesses (14μm) reduce their stiffness and allow them to buckle excessively before penetration. We are currently improving the resolution and sensitivity of our strain gauge system to allow the forces in penetrating pia to be quantified and may fabricate some of these probes with thicker substrates to allow further characterization of dura penetrations as well. The shallow-diffused sharp probe tips have recently proven to be much superior to the more rounded deep-diffused tips in penetrating the dural sheath surrounding Scarpa's Ganglion in the rat. We are also planning to perform the first simultaneous stimulation-recording experiments during the coming term to explore the use of "artificial neurons" in answering questions regarding tissue encapsulation of chronic recording sites. Calculations have shown that we should be able to limit crosstalk in these situations to less than ten percent of the recorded tissue voltages, making such measurements viable.

Tissue reaction was assesssed in three chronic stimulation experiments in which 1200-1600μm^2 sites were driven with charge-balanced anodic-first 50μA current pulses with 100μsec per phase. Seven to ten days following implantation there was 8 hours of stimulation a day for five days. Four weeks later the animals (guinea pigs) were perfused and histology was performed around the implant sites. Two of the 3-shank or 4-shank probes were in occipital cortex and the other probe was in cerebellum. Only minimal tissue reaction was observed in all three cases. A thin rim of gliosis was observed around the tracts except for a few cases where no glial sheath was observed around the tracts. There was no noticeable increase in reaction near the stimulation sites, at least not in the tissue that remained following removal of the probes. In a separate experiment with a similar stimulation protocol, however, two probe shanks were removed from tissue following the four-week post-stimulation period and were examined in an SEM. These probe shanks were very clean except for what appears to be adherent tissue on the active stimulating sites. No such tissue is seen on an adjacent unused (non-stimulated) site, and we are planning additional experiments to further investigate this situation.

A new computer-controlled system for site activation, deactivation, and cyclic voltammetry is also being developed using LabVIEW software. The system will offer the user control over a variety of parameters, will ensure reproducibility in the activation process, and will require minimal user interactions. We expect this system to be operational during the coming term.

A new run of active stimulating probes is in process, correcting problems noted in an earlier run. We plan to apply the resulting probes in-vivo during the coming term. These probes are capable of working with supply voltages as high as ±9V, which permits the 1000μm^2 sites to pass currents of approximately ±128μA in the face of tissue access resistance. The minimum supply voltages are now known for these probes as a function of the site area. At ±5V, access resistance precludes currents of much more than about 50μA through such sites. The final modifications are also being made to the external drive electronics for our active probes so that it will support in-vivo experiments during the coming term.

MICROMACHINED STIMULATING ELECTRODES

1. Introduction

The goal of this research is the development of active multichannel arrays of stimulating electrodes suitable for studies of neural information processing at the cellular level and for a variety of closed-loop neural prostheses. The probes should be able to enter neural tissue with minimal disturbance to the neural networks there and deliver highly-controlled (spatially and temporally) charge waveforms to the tissue on a chronic basis. The probes consist of several thin-film conductors supported on a micromachined silicon substrate and insulated from it and from the surrounding electrolyte by silicon dioxide and silicon nitride dielectric films. The stimulating sites are activated iridium, defined photolithographically using a lift-off process. Passive probes having a variety of site sizes and shank configurations have been fabricated successfully and distributed to a number of research organizations nationally for evaluation in many different research preparations. For chronic use, the biggest problem associated with these passive probes concerns their leads, which must interface the probe to the outside world. Even using silicon-substrate ribbon cables, the number of allowable interconnects is necessarily limited, and yet a great many stimulating sites are ultimately desirable in order to achieve high spatial localization of the stimulus currents.

The integration of signal processing electronics on the rear of the probe substrate (creating an "active" probe) allows the use of serial digital input data which can be demultiplexed onto the probe to provide access to a large number of stimulating sites. Our goal in this area of the program has been to develop a family of active probes capable of chronic implantation in tissue. For such probes, the digital input data must be translated on the probe into per-channel current amplitudes which are then applied to the tissue through the sites. Such probes require five external leads, virtually independent of the number of sites used. As discussed in our previous reports, we are now developing a series of three active probes containing CMOS signal processing electronics. Two of these probes are slightly redesigned versions of an earlier first-generation set of designs and are designated as STIM-1A and STIM-1B. The third probe, STIM-2, is a second-generation version of our high-end first-generation design, STIM-1. All three probes provide 8-bit resolution in setting the per-channel current amplitudes. STIM-1A and -1B offer a biphasic range using ±5V supplies from 0μA to ±254μA with a resolution of 2μA, while STIM-2 has a range from 0 to ±127μA with a resolution of 1μA. STIM-2 offers the ability to select 8 of 64 electrode sites and to drive these sites independently and in parallel, while -1A allows only 2 of 16 sites to be active at a time (bipolar operation). STIM-1B is a monopolar probe, which allows the user to guide an externally-provided current to any one of 16 sites as selected by the digital input address. The high-end STIM-2 contains provisions for numerous saftey checks and for features such as remote impedance testing in addition to its normal operating modes. It also offers the option of being able to record from any one of the selected sites in addition to stimulation.

During the past quarter, research on this contract has focused in several areas. We are now close to completing the development of instrumentation aimed at characterizing the influence of probe tip shape on the ability to penetrate the membranes over the brain and enter tissue with minimal tissue damage. Additional experiments in this area were performed during the past term. Additional work was also done on the characterization of sites in-vivo during and as the result of chronic stimulation. Histology has also been

performed on several past chronically stimulated implants. A new system for site activation is under development, and a new run of active stimulating probes is in process along with the final modifications on the external circuitry necessary to drive such probes in in-vivo stimulation protocols. The results in each of these areas are described below.

2. *Penetration Studies with Passive Stimulating Probes*

The penetration studies have been discussed in previous reports at length in terms of the design of the various probe geometries to be fabricated and tested. Briefly, a set of probes has been designed and fabricated incorporating different tip and shank geometries in order to study the tissue coupling, insertion forces, and tissue damage associated with inserting the probes through the pia arachnoid and dura mater of guinea pigs and other experimental animals. These probes were designed to help define the optimum probe shank geometry: one that will provide the best combination of low penetration force with minimal cortical surface dimpling, minimal tissue damage and/or reaction along the insertion track, and maximum tissue-electrode coupling.

During the past quarter, more work was done to study the force required for penetration of probes into neural tissue. Penetrations were performed with 6 different 10-shank 2-D probe arrays: an array with 200μm shank separations; an array with 400μm shank separations; and an array with 200μm shank separations with tapered shank lengths (see Fig. 1). Each array was realized in both shallow- and deep-boron-diffused tip configurations. The penetrations were controlled and the data was collected with a Macintosh IIx computer-based data acquisition system using LabVIEW software as described in the previous report. The arrays incorporated polysilicon strain gauges on three of the shanks in order to measure the penetration forces. The penetrations were performed in guinea pig cortex both with the dura mater intact and then with the dura mater and arachnoid removed leaving only the pia mater. The results were almost identical to those discussed in the previous report. Neither the deep boron-diffused tips nor the shallow boron-diffused tips were capable of penetrating the dura mater, while both were able to easily penetrate the pia mater. The shallow boron diffused (sharp) tip arrays penetrated the pia mater with no visible probe buckling, no measurable strain gauge resistance change, and with only the slightest visually perceptible cortical surface dimpling. This ease of penetration is very desirable but does not help us in quantifying the differences in force required for the penetration of the various tip shapes. We are currently making several instrumentation changes to our strain-gauge recording system that should increase our readout sensitivity and hopefully will raise the strain gauge signals well above the noise floor, allowing pia pentrations to be monitored quantitatively. The deep boron diffused probes penetrated the pia mater with only slightly more force required than the sharper shallow-diffused tips. The cortical dimpling was easily observable visually, while shank buckling was perceptible but not enough to cause a measurable change in the strain gauge resistance, at least not with the current readout setup. Again, the problem is that the measured signal is of the same amplitude as the noise of the present measurement system. A differential output configuration should reduce this noise level by allowing the system to focus only on resistance changes while avoiding the total voltage across the strain gauge.

Previous work by Najafi and Hetke demonstrated the ability to penetrate the dura mater with probes that had tips that were not as sharp as those tested in this study. The question arises then, why are these *sharper* probes unable to penetrate the dura mater? The answer appears to be that the currently used probe shanks themselves are not as stiff as those used in previous work simply because the shanks are much thinner. The probe

shanks used in the current studies are 14μm thick compared with up to 30μm in the previous work.

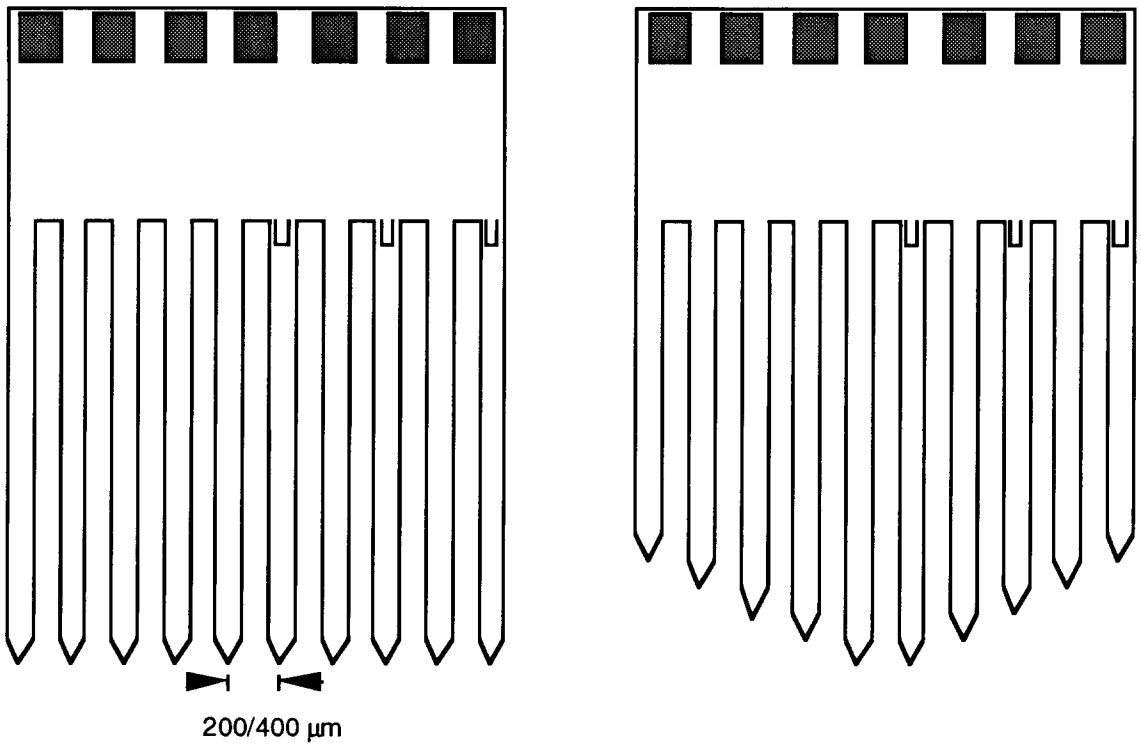

Fig. 1: The two array styles of 2-D 10-shank probe arrays.

The governing equation for an axially loaded column is

$$P = 2EI\pi^2/L^2$$

where P is the axial buckling load, E is Young's modulus (170GPa for silicon), L is the length of the column and I is the moment of inertia of the area as given by

$$I_{(Rectangular)} = Wh^3/12$$

for a rectangular column with width W and thickness h. This equation shows that the buckling load is proportional to the cube of the column thickness; therefore, a probe shank that is twice as thick will have a buckling load that is eight times greater. The present probes simply yield before penetrating the dura whereas the stiffness of the former probes was consistent with penetration.

As mentioned in the previous report, a closed form solution for the tip force on a buckled probe is very difficult to derive and requires the use of elastic theory; however, working with Prof. Noel Perkins (Mechanical Engineering and Applied Mechanics) and his student Chung-Long Lu, a numerical solution has been computed. The solution was computed in such a way as to provide a dimensionless relationship which could be used for any column by simply plugging in the proper geometric values. The relationship between the axial load and the tip displacement is fairly linear for tip displacements of up to one

fourth the length of the column. An interesting note is that the end load does not have to increase very much to cause a large change in tip displacement. In the case of our standard 14μm-thick, 65μm-wide 3mm-long probe shank, a force of 5.69×10^{-3}N is required to cause the shank to start buckling and a tip displacement of 25% of the shank length (0.75mm) only requires an 8% increase in the loading force to 6.18×10^{-3}N. This solution gives an upper bound on the force required for penetration of the pia mater with either the sharp or the blunt probe tips. The force required for penetration of the sharp tip is less than the buckling force and the force required for penetration of the blunt tip is very close to the buckling force. As we increase the measurement resolution of our current gauge readout system, we should obtain more quantitative information on these parameters.

Attempts to penetrate the dura mater with the 10-shank 2-D array probes provided a measurement of how the force is distributed throughout an array. Figure 2 shows the resistances of the three strain gauges versus microdrive position on an array of equal length shanks. The zero point on this graph is not the cortical surface but rather a reference point prior to probe contact with the brain. Strain gauge #1 is the end (outside) shank on the probe with #2 being on the third shank from the end and #3 being on the fifth shank from the end (see Fig. 1). As expected, the strain starts to build up in the outside shank first and then progresses toward the center. In order to minimize global cerebral dimpling, it is desirable to have adjacent shanks penetrate independently. Eventually measurements such as this in the pia will help provide a way to evaluate the necessary changes in shank length between neighboring shanks to achieve independent penetrations. In Fig. 2, the shanks buckle at about 1700μm, 2200μm, and 2500μm, giving an approximate profile to the depressed cortical surface.

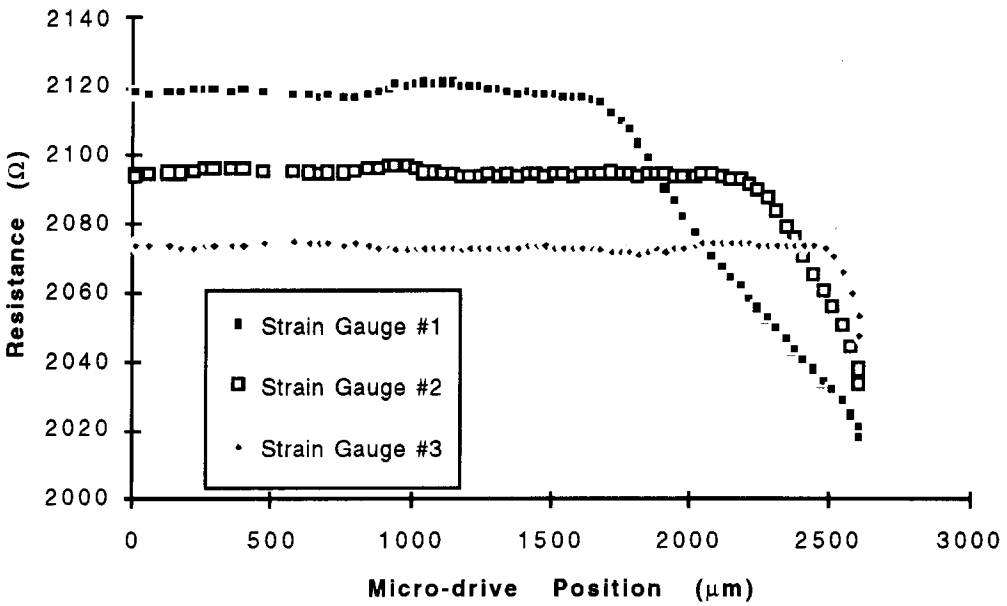

Fig. 2: Resistance of the three strain gauges of a 10-shank deep boron-diffused probe having lateral shank spacings of 200μm. All shanks here were of the same length.

The importance of tip design on the outcome of experiments was emphasized recently in our laboratory. The preparation involved penetration of the dural sheath covering Scarpa's Ganglion in the rat. Working in cooperation with a biomedical group at the NASA/AMES research laboratory to develop a chronic vestibular ganglion preparation,

we determined that the shallow boron-diffused tip structure was effective in penetrating this nerve sheath and preserving the viability of the tissue for unit recording. Other tips used on some of our older electrode designs (deep boron-diffused tips) were not nearly as effective at penetration and did not yield good unit recording results. One other new tip design was tested for its ability to penetrate and was also successful in penetration but no measure of recording quality was made. This was the first attempt at recording from ganglion neurons of a cranial nerve, and we are very encouraged by the outcome.

The development of LabVIEW software to perform chronic electrode encapsulation and tissue impedance experiments has also started. The ability to drive a signal into tissue and record from an adjacent electrode site without excessive crosstalk between the driven lead and the recording lead has traditionally been very difficult. In order to get an idea of what to expect, a equivalent circuit model was developed for the probe and its connector, and then the circuit was simulated via computer. The crosstalk was also estimated using hand calculations. The circuit model for the chronic passive probe is shown in Fig. 3. The crosstalk coupling between the stimulating and recording lines occurs primarily between the external leads that connect to the probe and to a much lesser extent through the bulk silicon substrate.

On the probe itself, direct capacitive coupling from the stimulating to the recording leads is thought to be negligible because of the silicon ground plane under the leads and the extracellular fluid conductor above them. The leads are separated by almost 30μm. However, one potential coupling path occurs due to capacitive coupling between the stimulating lead and the substrate, causing a slight voltage bounce on the substrate which is capacitively coupled back into the recording channel. Because of the low substrate resistivity and the high capacitive coupling to the quasi-neurtral extracellular fluid, however, this crosstalk is estimated at about 6ppm. For 1V on the stimulating electrode, this would represent a recorded crosstalk voltage that would be buried in the electrode noise. Thus, crosstalk will be limited to coupling between the external leads (shielded coax) and across the percutaneous plug itself.

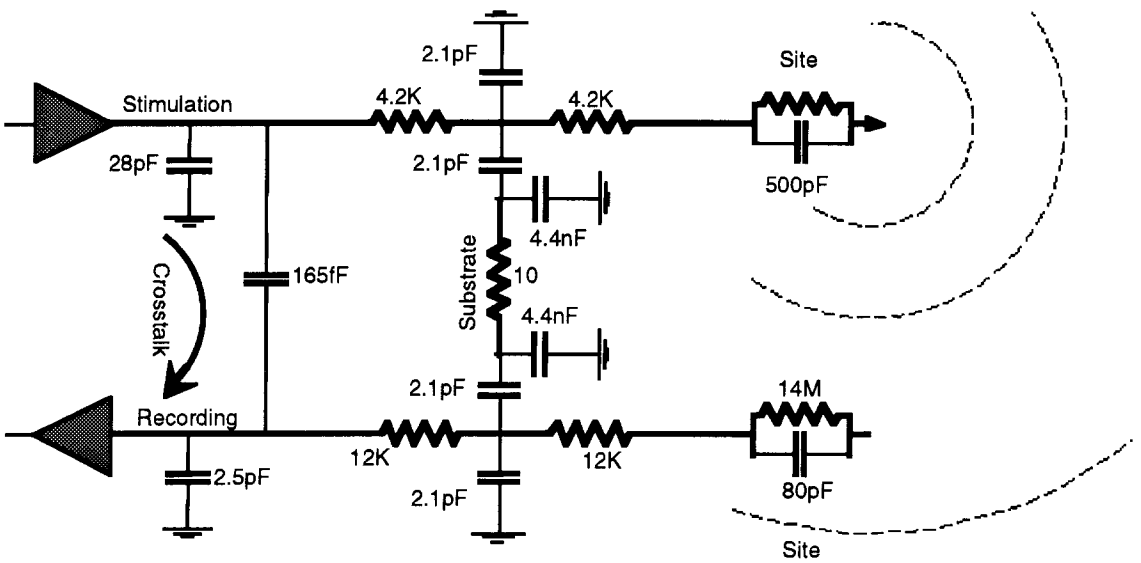

Fig. 3: Equivalent circuit for a stimulating and recording electrode pair, showing the elements important in assessing crosstalk.

In order to assess the feasibility of simultaneous recording and stimulation, it is important to estimate the voltage available in tissue due to the stimulation. The intent of these measurements is to provide an "artificial neuron" a short distance away from the recording site through supposedly undisturbed tissue so that we can assess whether tie site is being slowly encapsulated over time during a chronic implant or whether the neural circuitry is simply no longer active in the vicinity of the probe. Thus, we can tolerate some background level of crosstalk but would like it to be less than about ten percent of the signal recorded from tissue. For our present probes, the stimulating sites have an area of $1000\mu m^3$ and are 200μm from the recording sites (on an adjacent shank). If we take a rough model of the stimulating situation as equivalent to a spherical current field eminating from a spherical electrode surface having a radius of 9μm (equivalent to the actual surface area), then using a tissue resistivity of 600 ohm-cm (which matches our access resistance measurements for these probes in cortex) the estimated total access resistance in tissue for monopolar stimulation is about 53K ohms. At 50μA drive current, this would create an access voltage of about 2.65 volts and a total electrode voltage of 3-4 volts. This is close to what is seen at this current level with such electrodes. The fraction of this resistance between the recording site and a remote ground would be about 2.4K ohms, making the recorded voltage about 120mV. At 10μA, the recorded voltage would be about 24mV with a stimulating electrode drive signal of about 1V. Thus, to maintain the crosstalk at less than 10% of the recorded signal from tissue, the crosstalk should be no more than about 0.3%. For the recording probe noted above and in Fig. 3, this implies a maximum allowable crosstalk capacitance of about 240fF.

A calculation of the crosstalk capacitance across our percutaneous plug with short wires running to it predicts a crosstalk capacitance of about 165fF, whereas an actual measurement of this capacitance gives about 225fF for neighboring pins (worst case). Thus, it appears feasible with these probes to perform simultaneous recording and stimulation while limiting direct crosstalk to no more than 10% of the tissue signal. During the coming term we will make such measurements during acute experiments and will begin chronic implants of these structures to explore the long-term behavior of recording sites in vivo.

3. In-Vivo Current Flow and Impedance Studies

Another chronic stimulation implant experiment was completed during the past quarter, and histology results from three chronic implants were examined. SEM data from a chronically implanted probe was obtained. Tank tests were designed to study the effects of anodic bias on stimulation parameters (e.g., access voltage, impedance). Also, alternative methods for activating iridium were investigated.

Chronic Stimulation Waveforms

The chronic stimulation experiment run this quarter was similar to those reported previously and will be reviewed briefly here. A passive, three-shank stimulating electrode was used. On each shank was a pair of $1000\mu m^2$ sites. The sites were activated to $30mC/cm^2$. The electrode was implanted in the right occipital lobe of an adult guinea pig, and a recovery period of 7-10 days post-op followed. After this period, the pig was stimulated for 8 hours a day for five straight days. Constant current, bipolar stimulation was performed on two site pairs for four hours each. One site pair had sites that were on the same shank while the other pair had sites on different shanks. It is theorized that encapsulation of the shank may result in differences in electrical characteristics between

these two stimulation schemes. The stimulation waveform consisted of two biphasic pulses, 100μsec per phase. The leading pulse is anodic first followed 1msec later by a cathodic first pulse. This waveform was presented at 500Hz. The current magnitude was 10μA. The voltage drop across the site pair was recorded in response to the above waveform and to a 1kHz sine wave (for gain and phase measurements). An average of 100 records were taken. Records were saved at the beginning and end of the four-hour period and at 30 minute intervals during the stimulation.

The results of this experiment show an interesting phenomena that is thought to have been caused by a change in the iridium oxide. The impedance of the oxide seemed to have two states, high impedance and low impedance. Records of the site-to-site voltage drop in response to the current pulse waveform are shown for both cases below. These records are from one bipolar pair during a single four hour stimulation period, but both site pairs exhibited this behavior throughout the week of stimulation. It should also be noted that this is the only experiment to show this phenomena.

Site to Site Voltage Drop in Response to a Biphasic Current Pulse

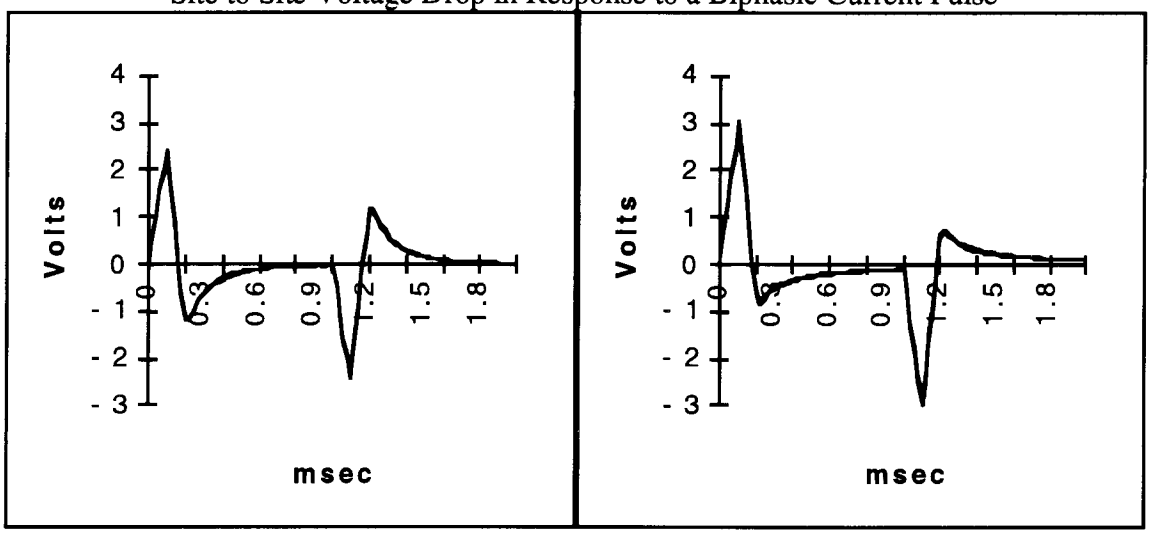

Fig. 4: Low Impedance State

Fig. 5: High Impedance State

The two figures (Figs. 4 and 5) each contain a series of records. Several statements can be made that lend credence to the theory that the impedance of the oxide, not the tissue, is changing. The electrical connections to the animal were intact. When the connection to the animal was purposely opened, a waveform different from the high impedance state resulted. Records of the same class are very similar. Also, from observations on an oscilloscope, the transition from one state to the other seemed somewhat abrupt. A low to high impedance transition would occur over a couple of minutes, with the scope display showing the impedance apparently toggling between the two states before settling on the high state. A high to low impedance transition would occur very abruptly and was usually triggered when the waveform was halted to take data. If tissue impedance were changing, one would expect a gradual change with more intermediate values.

The basic model of the electrode-tissue interface is a parallel capacitor-resistor combination in series with a resistor. When this network is excited with a biphasic current

pulse, the ideal waveform results (Fig. 6). The voltage across a capacitor discharging through a resistor is governed by

$$V(t) = V_0 * \exp(-t/\tau) \qquad \tau = R_e C_e$$

The rate at which the capacitor is discharged is determined by the capacitor and the resistor (i.e., by the time constant, τ). The time constants for the two waveforms were computed by analyzing the decaying tail of the waveform. The high impedance state was shown to have a longer time constant. This could be the result of either an increased R_e or C_e since $\tau = R_e C_e$. However, the V_e of the high impedance pulse is larger. This points to an increased R_e, since $V_e(t)$ is the voltage across a charging RC circuit and is given by

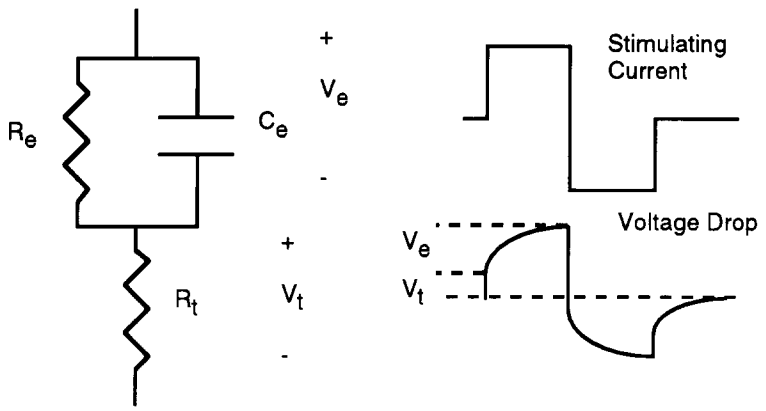

Fig. 6: Ideal model for the electrode-tissue interface

$$V_e(t) = I * R_e(1-\exp(-t/\tau))$$

Both site pairs displayed this phenomena. There were differences between this experiment and previous experiments, which did not show two-state behavior. The activation parameters for these electrode sites were altered slightly. The voltage limits of the activation ramp wave were lowered as was the charge capacity. These changes were a result of reviewing the study of iridium activation accomplished at EIC (discussed further below). Also, a stimulus drive of 10μA was used in this experiment instead of the 50μA used previously. In any case, it was difficult to obtain impedance and access voltage data to compare to previous experiments. Previous reports told of increasing impedance during the course of stimulation. The nature of this data did not allow a determination if that trend was followed. However, some comparisons can be made. When in the low impedance state, the site to site impedance (at 1kHz) ranged from 300K to 400K ohms and the site-to-site voltage drop in response to the 10μA biphasic pulse waveform ranged from 1.8 to 2.5V. These data are in the same range as values found in previous experiments.

Chronic Stimulation Histology

Tissue reaction was assesssed in three chronic stimulation experiments. Two three-shank probes and one four-shank probe were used. The test protocols for the 3-shank probes were similar to that described above except that current magnitude was 50μA. For the four shank probe, both bipolar pairs had sites on the same shank either 1200μm^2 or 1600μm^2 (sites in a pair had the same size) and stimulation was between sites on same

shank, not between shanks. Seven to ten days following implantation there was 8 hours of stimulation a day for five days. Four weeks later animals were perfused with 4% paraformaldehyde fixative. Brains were dissected away from the cranium, the position of the probes was noted, and the probes were withdrawn from the brain. Brains were then embedded in plastic and horizontal sections (at right angles to the electrode tracts) were cut, mounted on slides, and stained. The position of the probe and stimulation sites was estimated from the distance between tissue sections (12μm), the number of sections from the end of the probe tract, and the known geometry of the electrode.

Two of the probes (one four shank, Fig. 7; one three shank, Fig. 8) were in occipital cortex and the other probe (three shank, Fig. 9) was in cerebellum. Only minimal tissue reaction was observed in all three cases. A thin rim of gliosis was observed around the tracts except for a few cases where no glial sheath was observed around the tracts. It is possible that in some cases the glial reaction adhered to the probe and was removed along with the probe. There was no noticeable increase in reaction at the stimulation sites. Results below on EM of electrodes would suggest that there may have been increased reaction that adhered to the probes. Few reactive cells were observed and the neuropil adjacent to the tracts appeared normal. There was increased reaction at the base of the tracts (Fig. 10) as we have observed earlier in cases where probes were fixed external to the brain and brain pulsing resulted in constant movement of probes relative to the brain. In a previous report, we reported on one case of chronic stimulation where under similar conditions we observed severe tissue reaction, with loss of neurons, necrosis and many reactive cells. The present results suggest that the probes and stimulation conditions per se do not result in severe tissue reaction, and the causes of reaction in the first animal need to be determined.

Electrode Site Evaluations

Photos of an electrode that had been implanted in a guinea pig were obtained using a SEM (ISI DS-130). The probe shown below has 1000μm^2 sites and had been used in a chronic stimulation experiment. The experimental protocol was identical to that described above except that the current magnitude was 50μA. The animal was sacrificed 4 weeks after the completion of stimulation. Two of the three shanks were retrieved from the animal. On those shanks were three sites that were used for stimulation (Figs. 11-13) and one site that was not (Fig. 14). All four sites were treated the same prior to implantation. It appears that some type of material is adhering to or accumulating on the sites while leaving the rest of the probe clean. The one site that was not used for stimulation is tissue free. Other figures included are a side view of the site in Fig. 11 (Fig. 15) and a top view of a used site and an unused site on the same shank (Fig. 16). Others groups at Michigan have run long term pulse tests on iridium electrodes in saline solution. The results of those tests show a significant build up of iridium oxide on the site after approximately 1 billion pulses. The pulse count in our experiments is lower (around 75 million) but it is not unreasonable to expect some extra oxide to form. Alternatively, tissue could in some way be adhering to the sites as a result of stimulation. Further analysis is needed to determine the nature of the material on the sites. This is the first electrode from the current round of chronic stimulation experiments that has been examined in this manner. The data suggest a correlation between stimulation and a formation of some type of substance, probably adhering tissue, on the site. In the future, a greater effort will be made to retrieve electrodes intact from chronic preparations so that the findings presented here can be substantiated and explored further.

During the next quarter we plan to study the effects of activation parameters on the ability of the iridium oxide to maintain consistent electrical characteristics over the long

term. Conversations with Dr. Lois Robblee, and a review of her past work (Studies of the Electrochemistry of Stimulating Electrodes, Final Report, 1991) have highlighted several areas where our present activation procedure could be altered. Specifically, the above report suggests use of a square wave for activation and 0.3M Na_2HPO_4 for an electrolyte. The present method uses a ramp wave with Phosphate-buffered saline as an electrolyte. Also, the activation limit will be lowered. The new limit will be $30mC/cm^2$ versus the $100mC/cm^2$ used currently. Studies have shown that oxides activated to a high level of charge capacity will not maintain electrical characteristics, while those activated to a lower level can hold a constant level of charge capacity. The new lower limit will still allow a maximum current of 3mA for a 100μsec pulse on a $1000\mu m^2$ site. An anodic bias will be placed on the sites in a further effort to improve charge injection capability (this method was also learned from Dr. Robblee's report and from a conversation with Dr. Doug McCreery at HMRI).

Experiments will be run to study the importance of the above activation parameters for maintaining electrical characteristics. The stimulation protocol will be similar to that used in the chronic implants except these tests will be run in saline. Also, tests with an anodic bias will be run to compare the access voltage of biased and unbiased sites. The current source we use has been modified to include an adjustable bias voltage. Dr. Robblee's report suggests the use of 0.6V.

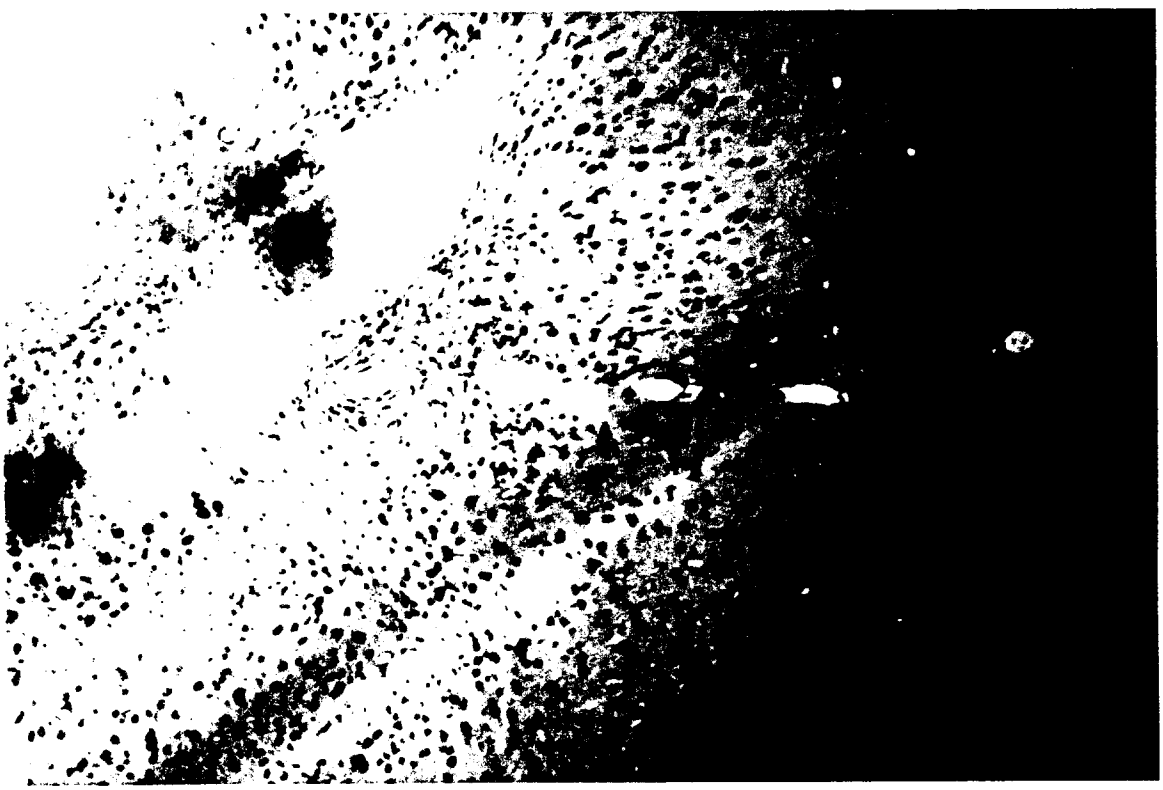

Fig. 7: Cortical tissue section of tracts of a three shank probe. 10X Mag.

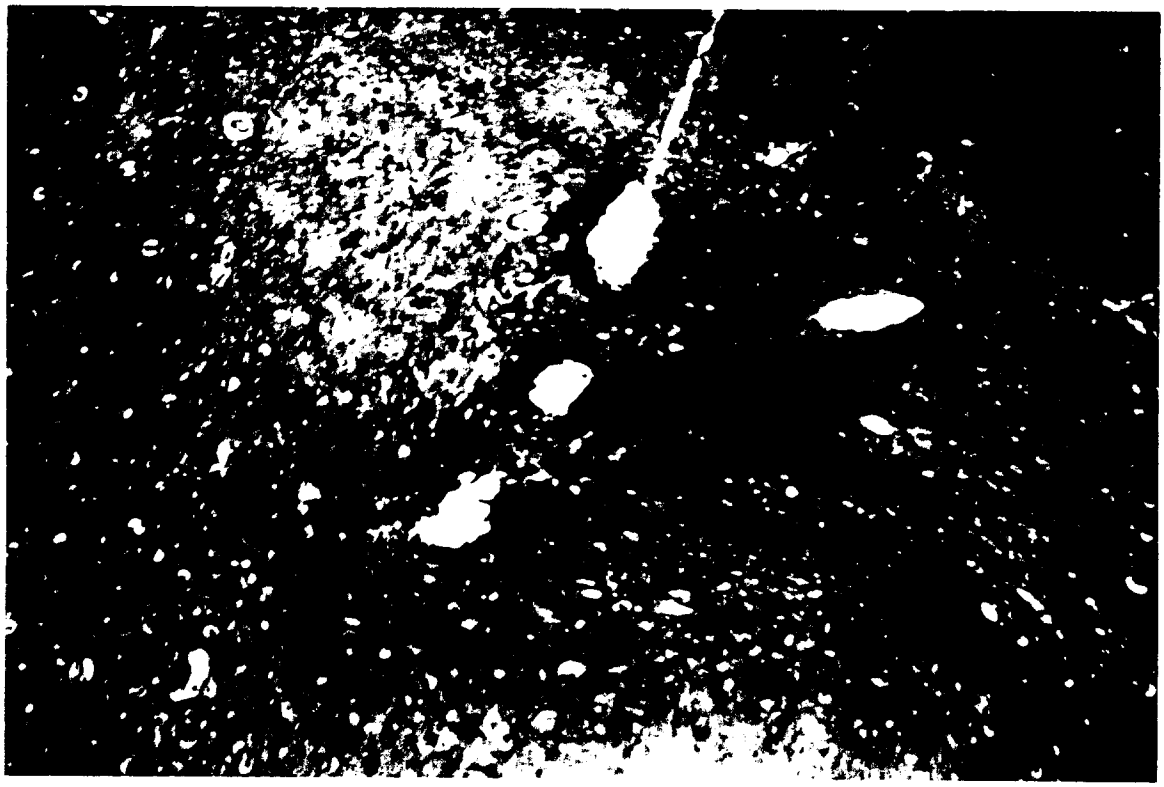

Fig. 8: Cerebellar tissue section of tracts of three shank probe. 10X Mag.

Fig. 9: Cortical tissue section of tracts of four shank probe. 10X Mag.

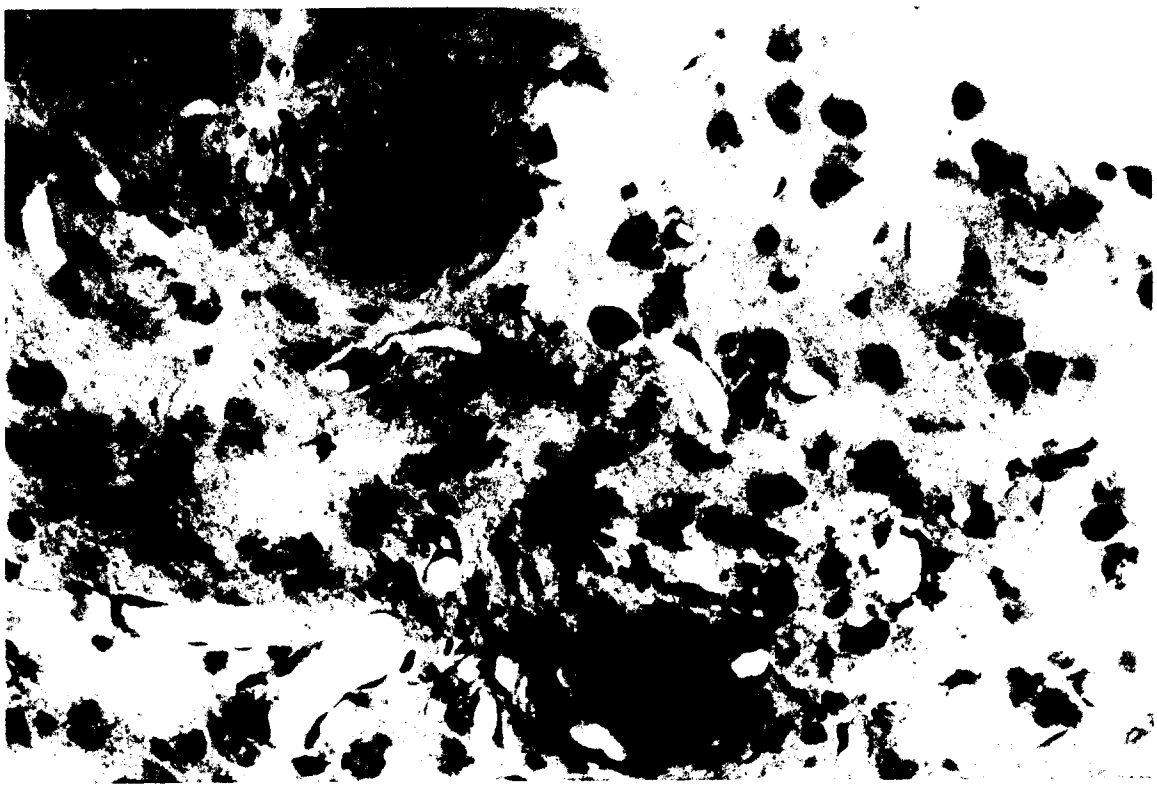

Fig. 10: Cortical tissue section of the area below the middle two shanks of a four-shank probe. 16X Mag.

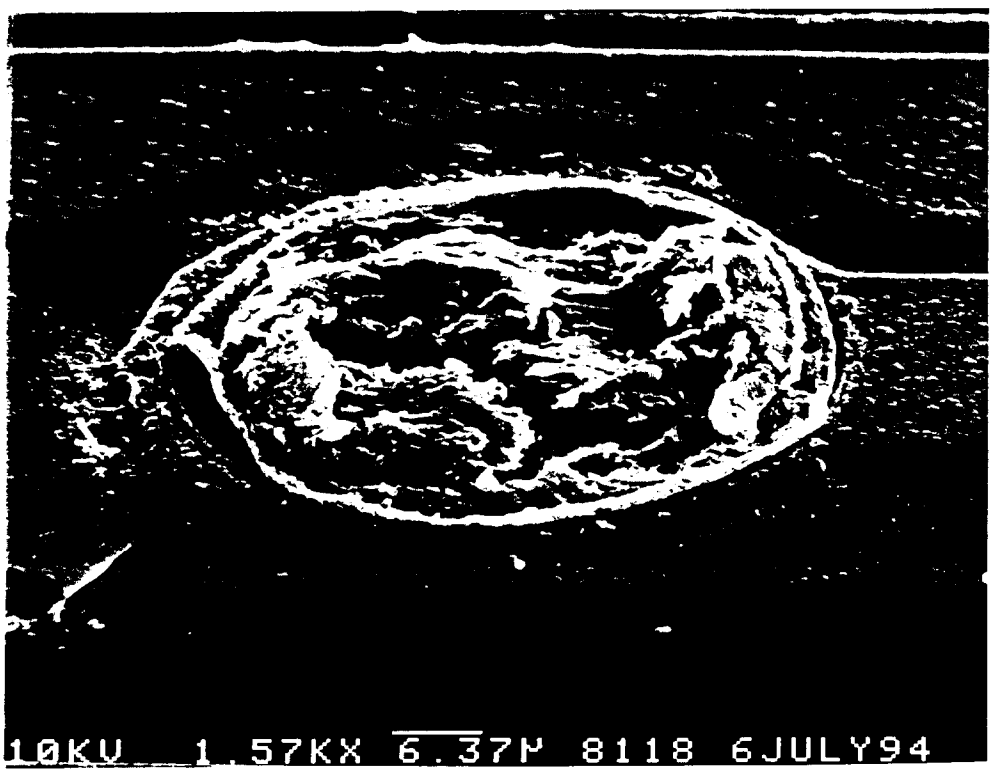

Fig. 11: Utilized site retrieved from a chronic implant.

Fig. 12: Utilized site retrieved from a chronic implant.

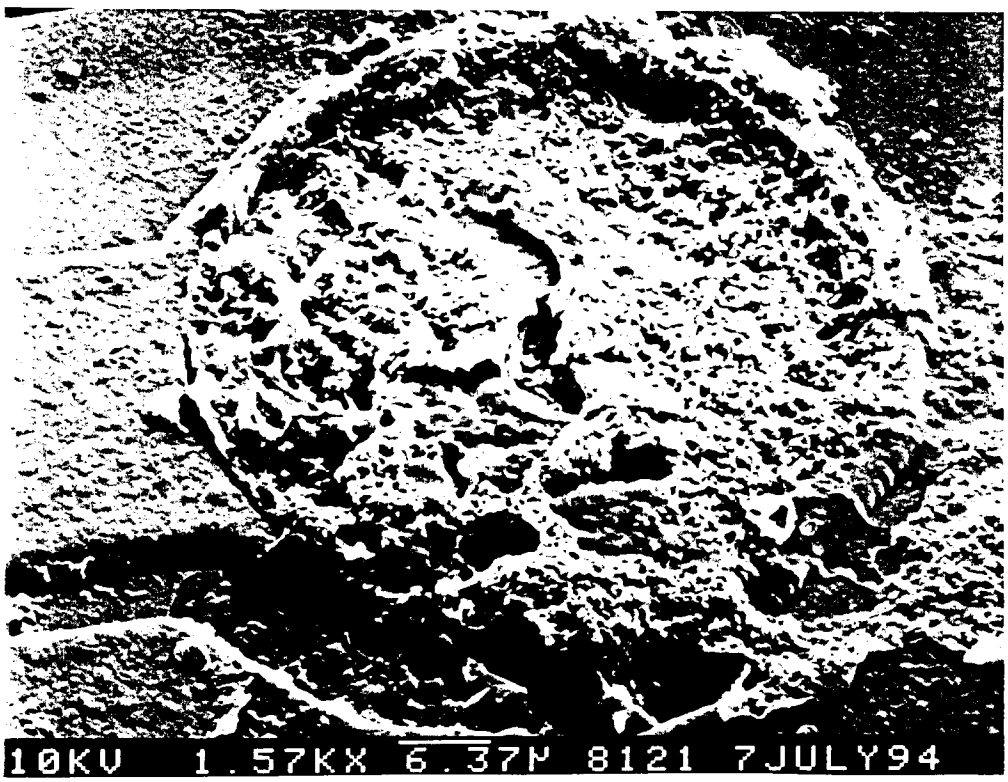

Fig. 13: Utilized site retrieved from a chronic implant.

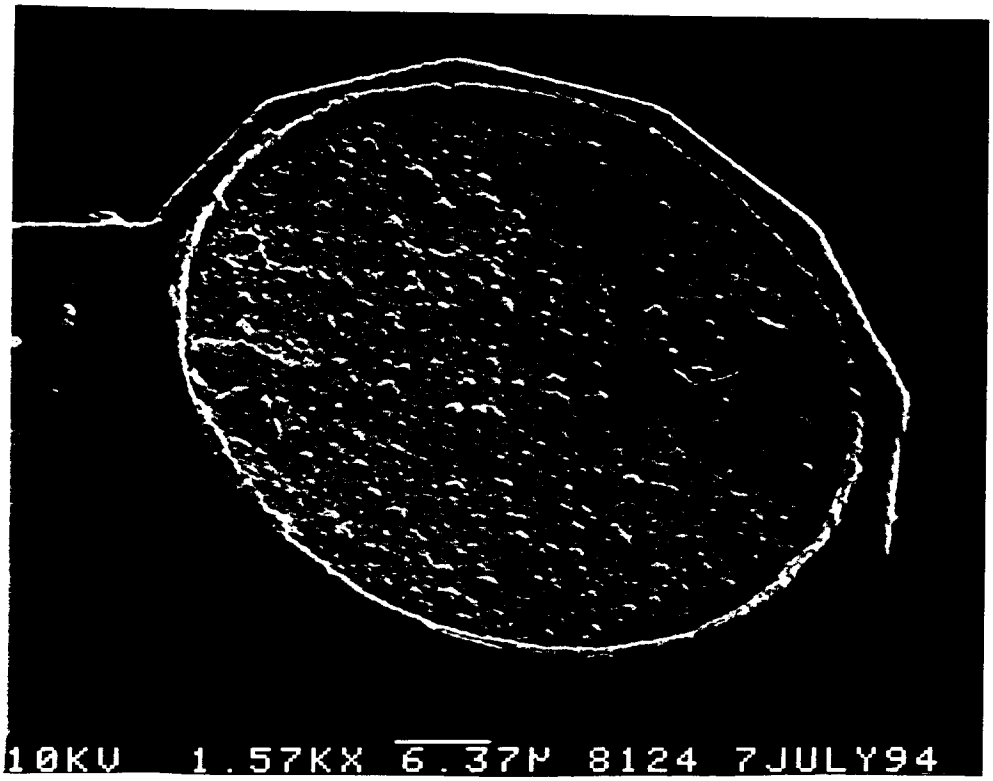

Fig. 14: Unused site retrieved from chronic implant.

Fig. 15: Side view of the site in Fig. 11.

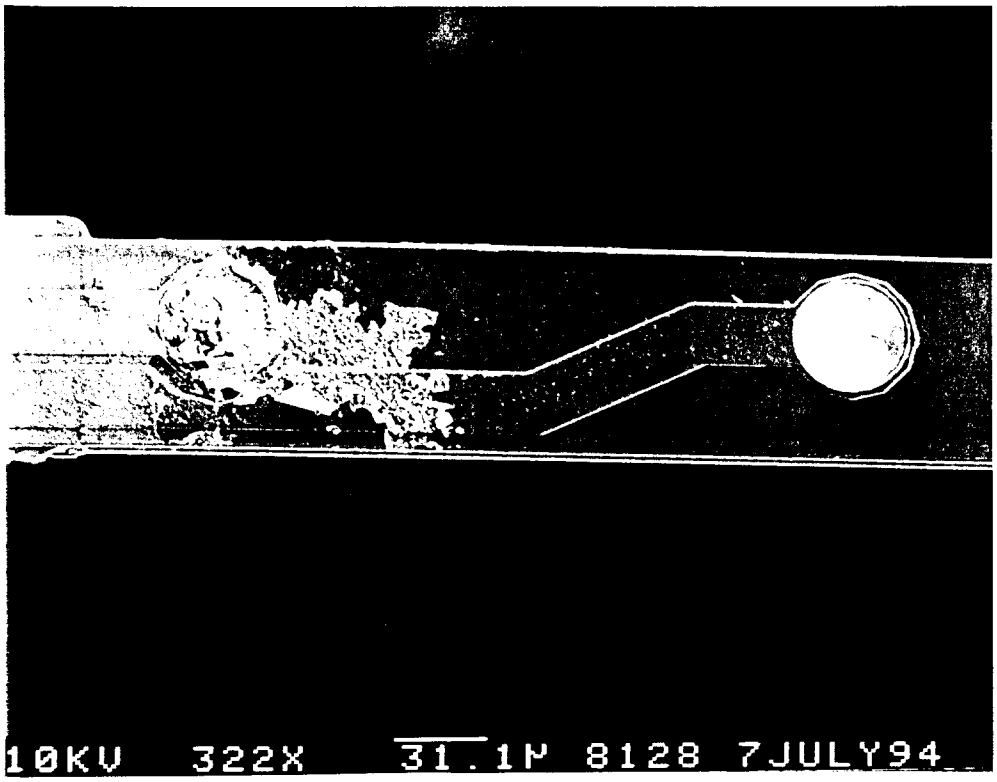

Fig. 16: Utilized and unused site on same shank

4. *A Software-Controlled Site Activation Station*

During the past quarter, work began on setting up a test station to grow anodically formed iridium oxide films (AIROFs) on the stimulating sites of multielectrode probe arrays. This test station is needed because the present system is unreliable. In addition, this station will provide more flexibility than the present system by allowing multiple sites to be processed without continual user interaction. This will allow all sites on a multielectrode probe array to be activated overnight. Hopefully, this test station will be completed during the next quarter.

This station will be capable of performing electrode site activation, deactivation, and cyclic voltammetry (CV). Site activation is the process of growing an oxide on the iridium site which is necessary for its use as a stimulating electrode. Site deactivation is the process of removing this oxide. Cyclic voltammetry measures the total charge capacity of the electrode site which, to a point, is a measure of the amount of oxide on the iridium site. Each of these processes can be performed on up to ten sites on a single probe without user interaction except for the initial setup.

Setting up this station requires software and hardware to be designed, implemented, and tested. LabVIEW, which is a graphical programming language, is used to implement the software. This software provides the user interface as well as the process control for the system. Initially, the user selects which process to run, the sites on which to run the process, and the appropriate parameters for the process such as voltage limits and sweep rate for the output wave and total charge capacity desired. The software sets up the data acquisition boards appropriately for the tests and sites selected, initiates the tests by

outputting waveforms using the D/A capabilities of the data acquisition boards, and collects data as necessary using the A/D on the data acquisition boards. The software then processes the data and displays the results for the user which, depending on the process selected, may include CV graphs and total charge capacity for each site selected.

Hardware controlled by the data acquisition boards physically connects and disconnects electrode sites from the appropriate circuits as determined by the user's selections in the initial setup. Other hardware smooths and buffers the output waveform from the D/A before it is passed to the solution that contains the electrode array. Signals passing through the selected sites are amplified and filtered before being input to the A/D. A reference voltage from a calomel electrode in the solution is buffered and input to the A/D as well. Figure 17 below shows a block diagram of the test station.

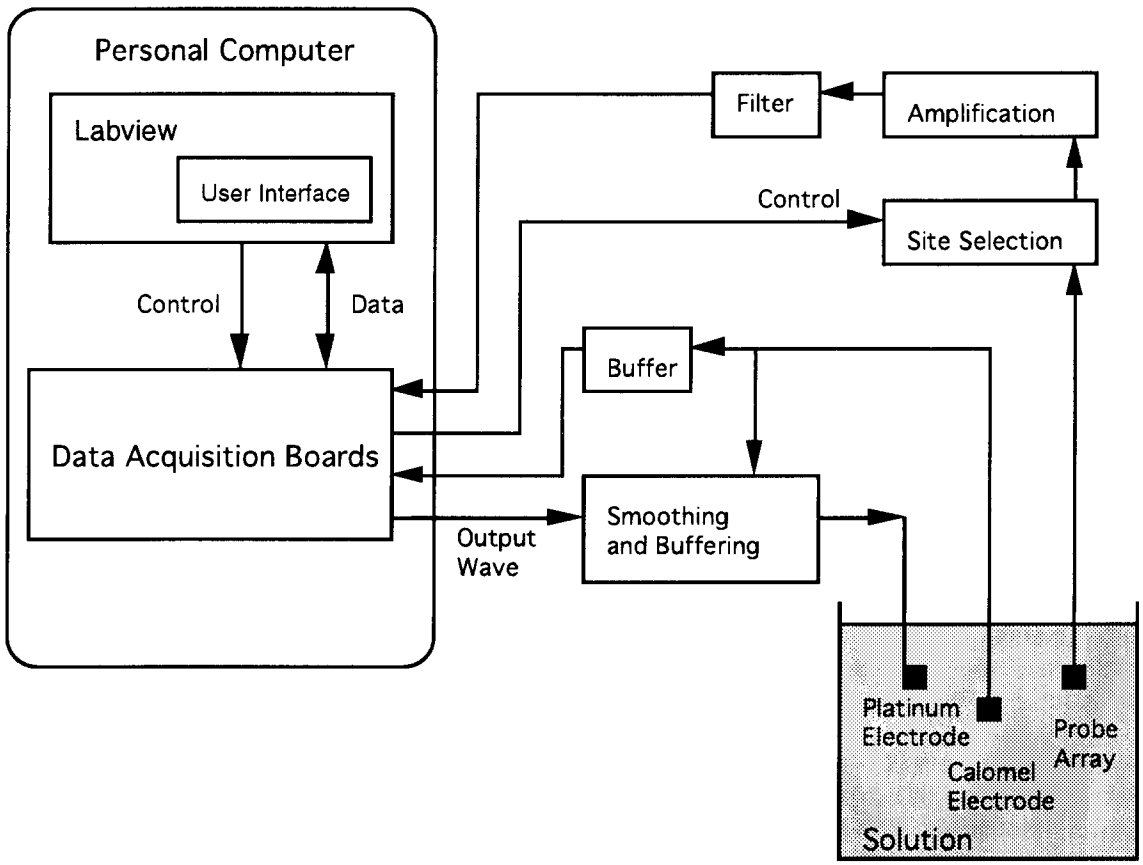

Fig. 17: Block diagram showing the new test station that will be capable of activating multiple sites without continual user interaction.

5. *Development of Active Stimulating Probes*

During the past quarter, we have started a new processing run of active stimulating probes. These probes have been aligned slightly (10°) off the crystallographic <110> axes to reduce the rather ragged edges produced on the circuit area edges in the last process run while still ensuring adequate undercut of the ribbon cables on some of these probes. As of this writing, the devices are at the p-well implantation stage, and we expect the probes

(including STIM-1a, -1b, and -2) to be finished during the coming quarter. At that time, we hope to use them in-vivo, probably for acute auditory experiments in the cochlear nucleus. Also during the present quarter, Dr. Changhyun Kim completed his doctoral thesis on the development of STIM-2. He will be staying at Michigan for an additional year to supervise the completion and application of this generation of active stimulating probes.

During the past quarter, we have taken another look at the minimum supply voltage requirements for neural stimulation in terms of the site size and other parameters. The supply voltage must be large enough to ensure that the intended current/charge levels can be delivered to tissue. This supply voltage is primarily limited by the logic circuit configuration used, the design of the probe, and the conditions under which it is operated, including the electrode site impedance and the resistivity of the tissue around the sites. It is important to know the lower limits on the operating supply voltage for a specific application in order to operate the system with the minimum power dissipation and with the lowest possible voltage stress across the encapsulating dielectrics.

The access voltage resulting from ohmic losses in the circuit-site-tissue system is primarily due to the electrolyte resistance close to the electrode. It is not included in the potential difference across the electrode-electrolyte interface that drives the charge transfer processes but it significantly limits the system operating voltage as the stimulating site becomes smaller. From a circuit aspect, if BiCMOS process technology is used, then the power supply voltage can be reduced to about ±1.3V. This includes contributions of about ±0.3V for the minimum drop across the output bipolar current sources (the bipolar saturation voltage) and about ±1V across the water window at the site-solution interface. This neglects any resistive drop in the tissue and so is valid only for large site areas. To confirm these values, measurements were made of the iR access voltage-drop (ViR) as a function of site area both in carbonate buffered saline (CBS) solution and in the cortical tissue of a rat. Also, calculations were made of the effective tissue resistance using a hemispherical model with the assumption of uniform ion density in the solution. In this model, the access resistance is proportional to the tissue resistivity and inversely proportional to the square root of the site area. The calculated values of this resistance in CBS using the hemispherical model are a good match to experimental measurements with a dispersion angle of 70° and a tissue resistivity of r=100Ω•cm. Using these values, the access voltage-drop (ViR) in CBS solution (or tissue) can be estimated as a function of site area. An access voltage-drop of about 1.1V was observed in CBS for a site area of 1000μm^2 and stimulating current of 100μA. This voltage-drop increased to 2.5V for a site area of 400μm^2. In tissue, the voltage-drop is about six times greater than in CBS, indicating an effective tissue resistivity of about 600Ω•cm. Therefore, the access voltage-drop in tissue (i.e., the tissue resistance) is critically important in determining the minimum power supply voltage for a given probe. At 1000μm^2 and 100μA, the iR drop in tissue is about 6.6V, increasing to about 15V for 400μm^2 and 100μA. If the advantages of low-voltage operation are to be fully utilized, either the size of the electrode sites must be increased or the stimulus amplitude should be decreased. In terms of overall probe size, and we suspect spatial localization of current, there is relatively little difference (only about 12μm in width) between a 400μm^2 site (20μm x 20μm) and a 1000μm^2 site (about 32μm x 32μm). In addition, the thresholds for neural activation observed in auditory tissue have been reported to be about 5-15μA, at least in terms of near field neurons. More sites should also make operation at lower levels of current per site possible.

Including the drop across the active current sources, the water window, and resistive drops in the tissue, the minimum allowable site area is about 700μm^2 for a supply voltage of ±5V and a stimulus current of ±50μA. Conversely, the lower limit of the power

supply voltage for an active stimulating probe is about 8V for a site area of 1000μm^2 and a maximum stimulating current of ±100μA. This calculated voltage is much higher than normal CMOS operating supply voltages (±5V) but is compatible with the present probe, which has an upper voltage limit of about 9V. A more attractive option would be the use of ±50μA with sites at least 2000μm^2 in size. Figure 18 shows the minimum power supply voltage as a function of site area for various stimulating current levels. In this calculation, a tissue resistivity of 600 Ω•cm, a water window of ±1.0V, and a BiCMOS DAC (VCEsat of 0.3V) are assumed. If we want to keep the supply voltage as ±5.0V, then the maximum stimulating current is limited to about ±70μA for the 1000μm^2 sites on STIM-2.

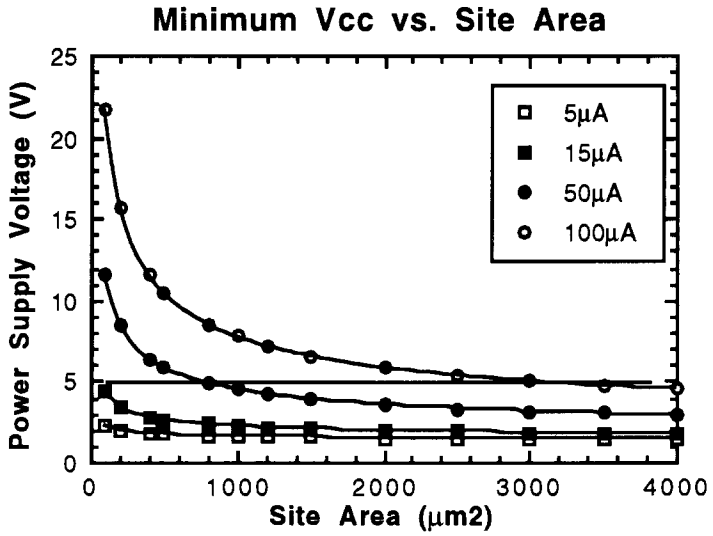

Fig. 18: Minimum supply voltage as a function of site area for various stimulating current level.

6. External Electronics for Active Stimulation Probes

In order to fully utilize the active probes, an external electronic system is necessary to format and feed desired pulse-pattern information to the probe. This system has been in development for some time, with the effort paralleling the development of the probes themselves. The previous quarter saw progress mainly in the area of the remote converter design. The PC daughterboard component of the external electronics remains stable and fully functioning. All of the issues regarding the design of the remote converter, such as the binary-to-ternary conversion, have been resolved. For the binary-to-ternary conversion, a set of analog switches will be used to select between the three driving voltages, with great care taken to prevent glitches and to protect against damage in case of an invalid set of binary inputs.

The final design of the remote converter is shown in block-diagram form in Fig. 19. Features of the design include complete isolation between the probe circuitry and the daughterboard circuitry. This isolation is achieved by using a separate power supply for the two components as well as opto-isolators in the interface between the two components. The electrical isolation will prevent line noise from reaching and possibly damaging the probes.

The basic remote converter circuitry (without isolation) has been implemented and tested on a breadboard as a verification of the design. The circuitry functions as expected except for some minor problems which are most likely caused by the large capacitive loads of the breadboard itself. The complete remote converter circuitry has recently been constructed on a wire-wrap board and is currently being tested. It is expected that the wire-wrap circuit will not suffer from the capacitive loading effects of the breadboard circuit and will therefore operate correctly.

In the coming quarter, it is expected that the remote converter will be fully tested, debugged, and integrated with current samples of the STIM-2 probe processor. This effort will mark the completion of the hardware construction component of the external electronics. The focus will then shift to the development of software drivers for the daughterboard circuitry. Currently, the software that exists is suitable only for basic testing. A more flexible and robust user interface will be developed.

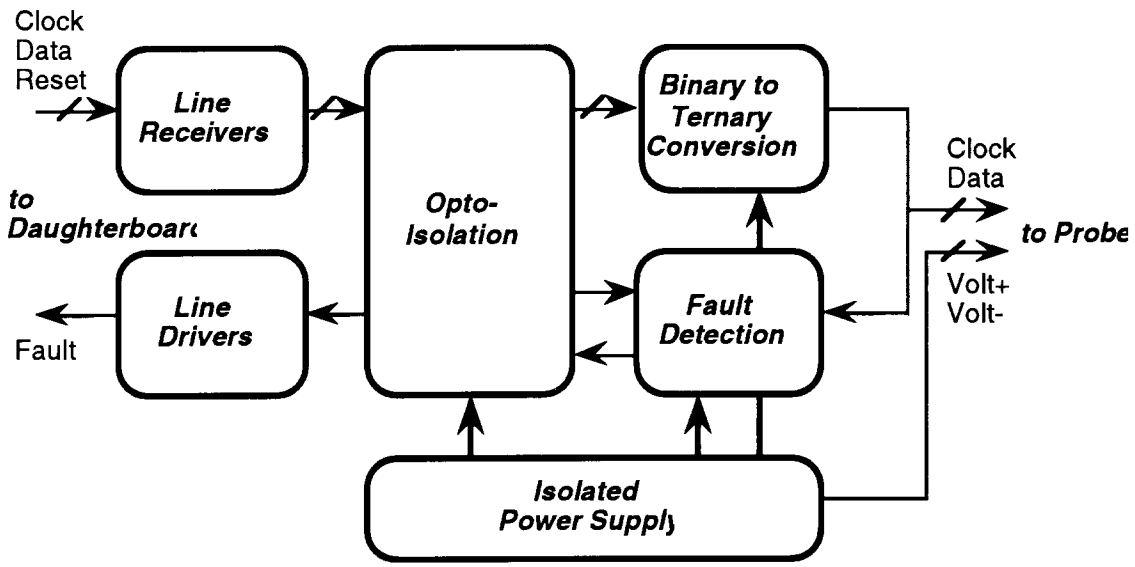

Fig. 19: Block diagram representation of the remote converter circuit.

7. *Conclusions*

During the past quarter, research under this program has focused in several areas. We have continued to produce a variety of passive stimulating probes and provide them to internal and external users. Additional experiments have been performed in penetrating the pia and dura with both single-shank and ten-shank probe structures. Both probes with shallow-diffused (sharp) tips and probes with deep-diffused (blunt) tips penetrate the pia mater with little discernable cortical dimpling and yield outputs that are below the ability of our present strain-gauge monitoring system to quantify them. None of these probes have successfully penetrated dura mater since their present thicknesses (14μm) reduce their stiffness and allow them to buckle excessively before penetration. We are currently improving the resolution and sensitivity of our strain gauge system to allow the forces in penetrating pia to be quantified and may fabricate some of these probes with thicker substrates to allow further characterization of dura penetrations. The shallow-diffused sharp probe tips have recently proven to be much superior to the more rounded deep-diffused tips in penetrating the dural sheath surrounding Scarpa's Ganglion in the rat. We

are also planning to perform the first simultaneous stimulation-recording experiments during the coming term to explore the use of "artificial neurons" to answer questions regarding tissue encapsulation of chronic recording sites. Calculations have shown that we should be able to limit crosstalk in these situations to less than ten percent of the recorded tissue voltages, making such measurements viable.

Tissue reaction was assesssed in three chronic stimulation experiments in which 1200-1600μm^2 sites were driven with charge-balanced anodic-first 50μA current pulses with 100μsec per phase. Seven to ten days following implantation there was 8 hours of stimulation a day for five days. Four weeks later the animals (guinea pigs) were perfused and histology was performed around the implant sites. Two of the 3-shank or 4-shank probes were in occipital cortex and the other probe was in cerebellum. Only minimal tissue reaction was observed in all three cases. A thin rim of gliosis was observed around the tracts except for a few cases where no glial sheath was observed around the tracts. There was no noticeable increase in reaction near the stimulation sites, at least not in the tissue that remained following removal of the probes. In a separate experiment with a similar stimulation protocol, however, two probe shanks were removed from tissue following the four-week post-stimulation period and were examined in an SEM. These probe shanks were very clean except for what appears to be adherent tissue on the active stimulating sites. No such tissue overgrowth is seen on an adjacent unused (non-stimulated) site, and we are planning additional experiments to further investigate this observation.

A new computer-controlled system for site activation, deactivation, and cyclic voltammetry is also being developed using LabVIEW. The system will offer the user control over a variety of parameters, will ensure reproducibility in the activation process, and will require minimal user interactions during the activation process. We expect this system to be operational during the coming term.

A new run of active stimulating probes is in process, correcting problems noted in an earlier run. We plan to apply the resulting probes in-vivo during the coming term. These probes are capable of working with supply voltages as high as $\pm$9V, which permits the 1000μm^2 sites to pass currents of approximately $\pm$128μA as designed in the face of tissue access resistance. The minimum supply voltages are now known for these probes as a function of the site area. At $\pm$5V, the access resistance precludes currents of much more than 50μA through such sites. The final modifications are being made to the external drive electronics so that it will support in-vivo experiments during the coming term.